Letters in Applied NanoBioScience
Open-Access Journal (ISSN: 2284-6808)

Article
Volume 15, Issue 1, 2026, 32
https://doi.org/10.33263/LIANBS151.032

Exploring the Antimicrobial Efficacy of *Pseudevernia furfuracea*: Phytochemical Analysis, *In vitro* Evaluation, and Molecular Docking Insights

Sharad Bhandarkar [1,*], Dr. Deepak Mohale [1], Dr. Anil Chandewar [1], Dr. Nitin Kochar [1], Dr. Krishnakant Bhelkar [2]

[1] P. Wadhwani College of Pharmacy, Yavatmal; bhandarkarsharad36@gmail.com (S.B.); deepak.mohale@gmail.com (D.M.); avchandewar@rediffmail.com (A.C.); nitinkochar01@gmail.com (N.K.);
[2] Gurunanak College of Pharmacy, Nagpur; krishnakant_bhelkar@rediffmail.com;
* Correspondence: bhandarkarsharad36@gmail.com;

Received: 30.08.2024; Accepted: da24.02.2026te; Published: 30.03.2026

Abstract: The growing resistance of bacteria to conventional antibiotics necessitates the exploration of natural sources for novel antimicrobial agents. *Pseudevernia furfuracea* (*PF*), a lichen species, has been traditionally used for its medicinal properties, but its antibacterial activity against common pathogens is poorly documented. This study evaluated the antibacterial activity of *PF* extracts against *S. aureus* and *E. coli* using the agar well diffusion method, and compared their efficacy with that of the standard antibiotic Gentamicin. The methanolic extract of *PF* exhibited the highest antibacterial activity, with zones of inhibition measuring 25 mm, 27 mm, and 29 mm against *E. coli* and 14 mm, 18 mm, and 25 mm against *S. aureus* at concentrations of 25 µl, 50 µl, and 100 µl, respectively, as compared to other extracts. Molecular docking revealed favorable binding affinities between *PF* phytoconstituents and *E. coli* Gyrase B, suggesting a potential mechanism of action. The study underscores the potential of *Pseudevernia furfuracea* as a promising source for natural antibacterial agents, with future applications in clinical settings and pharmaceutical development. Further research is warranted to explore its full therapeutic potential.

Keywords: *Pseudevernia furfuracea*; antibacterial activity; methanolic extract; agar well diffusion; molecular docking; natural antimicrobial agents.

1. Introduction

Antibiotic-resistant pathogens like *Escherichia coli* and *Staphylococcus aureus* are leading causes of severe infections worldwide, posing significant public health challenges. This growing resistance highlights the urgent need for alternative antimicrobial agents. Lichens are fascinating organisms formed by a partnership between a fungus and an alga or cyanobacterium. This unique relationship allows them to thrive in a variety of environments, from the cold Arctic to tropical rainforests, and even on bare rocks [1]. This symbiotic relationship enables lichens to persist in extreme conditions where few other organisms can live. Because of their resilience, lichens play an important role in ecosystems by helping to form soil, recycling nutrients, and creating habitats for other living things. Their ability to thrive in different environments makes them key indicators of environmental health and change.

Studying lichens provides valuable insights into how living things adapt and survive in nature [2].

Lichens absorb nutrients from the air, rainwater, and the surfaces on which they grow, making them excellent indicators of environmental health, especially air quality. Because they are sensitive to pollution, scientists use lichens to monitor the health of ecosystems. Lichens reproduce both sexually, through spores, and asexually, by breaking off into pieces that grow into new lichens [3]. With over 20,000 species, lichens come in different forms, such as crusty, leafy, or shrubby types. They play a crucial role in nature by helping to break down rocks into soil, providing food and shelter for wildlife, and enriching the soil with nitrogen. Their importance to biodiversity and ecosystem health cannot be overstated [4].

Some lichen species, like *Stereocaulon tomentosum*, *Pseudevernia furfuracea*, *Cetraria islandica*, *Evernia prunastri*, *Lobaria pulmonaria*, *Xanthoria elegans*, and *Umbilicaria hirsuta*, are well-known for their medicinal properties [5]. PF is less studied, even though it shows great potential. Recent research suggests that PF has strong anticancer [6], antimicrobial, anti-inflammatory, and antibacterial properties, making it a promising candidate for the development of natural medicines [5,7]. Although not as widely studied as other lichens, its bioactive compounds could be valuable for developing natural remedies.

Pseudevernia furfuracea (*PF*), commonly known as "tree moss" or "lichen moss," usually grows on the bark of coniferous trees in temperate regions [8]. It has attracted scientific attention for its strong antimicrobial, anti-inflammatory, and antibacterial properties, which are linked to its rich content of bioactive compounds, such as usnic acid, depsides, and depsidones [9–11]. These compounds have been shown to effectively inhibit the growth of various microorganisms, including bacteria, viruses, and fungi [12]. *PF* has shown particularly strong antibacterial effects against both Gram-positive and Gram-negative bacteria, making it a promising natural alternative to traditional antibiotics, especially given the growing issue of antibiotic resistance. Overall, *PF* shows great promise for developing new natural products for health and medicine, particularly for controlling infections and managing inflammation. Its bioactive compounds could lead to new treatments for cancer and chronic inflammatory conditions.

To fully understand and confirm the mechanisms by which the bioactive compounds in *PF* exert their antimicrobial activity, in silico molecular docking studies are a crucial step for elucidating the interactions between the phytoconstituents and bacterial proteins involved in vital processes such as cell wall synthesis, DNA replication, and protein production [13]. This approach not only validates the antimicrobial potential of *PF* but also accelerates the development of novel natural products that could serve as alternatives to conventional antibiotics, particularly in the fight against antibiotic-resistant bacteria.

Overall, integrating in silico molecular docking studies with experimental findings on PF antimicrobial activity is essential for confirming the mechanisms of action of its phytoconstituents. This approach will deepen our understanding of how these compounds work and support the development of new natural products with significant therapeutic potential. Thus, the present study was designed to investigate the antimicrobial efficacy of PF's active metabolites.

2. Materials and methods

2.1. Collection and authentication of lichen.

The lichen thallus was collected from Nagzira Wildlife Sanctuary, Tirora Goregaon Tahsil, District Gondia, Maharashtra, India, in February 2023. The sample was then sent for authentication to the Council of Scientific and Industrial Research (CSIR) - National Botanical Research Institute, Lucknow, Uttar Pradesh. The voucher specimen, numbered PDSH/LWG/Authentication/2023-24/14, dated 7/06/2023, was deposited at the institute.

2.2. Lichen extracts preparation.

Twenty-five grams of air-dried *PF* thallus, including both vegetative and fruiting bodies, were thoroughly washed and dried. The dried thalli (22 g) were then subjected to successive solvent extraction using a Soxhlet apparatus, following the previously described method [14]. The extraction began with petroleum ether (60-80°C), followed sequentially by chloroform, acetone, and methanol. The extracts obtained were concentrated using a rotary evaporator and subsequently used for further phytochemical and pharmacological evaluations.

2.3. Phytochemical screening.

Freshly prepared Lichen extracts were analyzed for the presence of various phytochemicals such as flavonoids, saponins, alkaloids, carbohydrates, proteins, and tannins, using standard methods as described previously [15].

2.4. Antibacterial activity.

The antibacterial potential of *PF* extracts was evaluated using the Kirby-Bauer well diffusion method [16]. Freshly grown bacterial cultures, standardized to 0.5 McFarland turbidity, were prepared from 24-hour nutrient broth cultures of *S. aureus* (Gram-positive) and *E. coli* (Gram-negative). These cultures were inoculated onto sterile, solidified Muller-Hinton Agar (MHA, HIMEDIA-M173) plates using the lawn culture technique with sterile cotton swabs [17]. Stock solutions of each extract were prepared at a concentration of 1 mg/ml. Three wells (8 mm in diameter) were bored into the MHA plates using a sterile cork borer, and each well was filled with 25 µL, 50 µL, and 100 µL of the extract solution. The plates were allowed to stand at room temperature for 2-3 hours to facilitate diffusion, after which they were incubated in an upright position at 37°C for 24 hours. The zones of inhibition around each well were measured to assess antibacterial activity. The zone of inhibition was calculated by measuring the diameter of the clear area surrounding each well in millimeters (mm). Control plates were prepared using 100 µL of DMSO as a negative control, and gentamicin was used as a positive control.

2.5. Molecular docking.

Computational docking studies of phytoconstituents from *PF* were performed using AutoDock Vina software [18,19]. The analysis utilized the 1.90 Å crystal structure of *E. coli* Gyrase B 24kDa (PDB ID: 6F86), obtained from the Protein Data Bank (https://www.rcsb.org). The structure included the inhibitor 4-(4-bromo-1H-pyrazol-1-yl)-6-[(ethyl carbamoyl) amino]-N-(pyridin-3-yl) pyridine-3 carboxamide, with an R-Value Free of 0.219 and an R-

Value Work of 0.203. For docking preparation, chain A was selected, and non-standard residues were removed. Energy minimization and geometry optimization were conducted using UCSF Chimera's Dock Prep tool. Gasteiger charges, polar hydrogens, and partial charges were assigned to ensure proper protonation at physiological pH [20]. Two-dimensional (2D) structures of the phytoconstituents were sourced from the NCBI PubChem database (https://pubchem.ncbi.nlm.nih.gov) and converted to three-dimensional (3D) structures using the Marvin program. Energy minimization of the ligands was performed with the Amber ff12SB force field in UCSF Chimera. Docking studies evaluated interactions between the phytoconstituents and 3CL protease, with binding energies calculated for protein-ligand complexes. AutoDock Vina, integrated with UCSF Chimera v1.14,used default parameters with a grid box of 15 × 15 × 15 Å, centered at (61.680, 28.331, 64.290) Å. Binding affinities were analyzed using the View Dock tool, and results were visualized with Discovery Studio 2020 Client and PyMOL [21,22].

3. Results and Discussion

3.1. Extraction of lichen.

The extraction process for the collected thallus was meticulously conducted using a Soxhlet apparatus with successive solvent extractions, which enabled the efficient isolation of bioactive compounds from the lichen thallus. The solvents were selected based on their increasing polarity to ensure comprehensive extraction of both non-polar and polar bioactive compounds. The successive extraction approach allows systematic separation of compounds based on their solubility, thereby maximizing recovery of bioactive metabolites. Starting with petroleum ether, followed by chloroform, acetone, and methanol, the extraction yielded varying amounts of extracts, which are indicative of the solubility and abundance of the lichen's constituents in each solvent. The yields were 2.5% w/w for petroleum ether, 3.5% w/w for chloroform, 4.5% w/w for acetone, and 7.5% w/w for methanol. The higher methanol yield suggests that polar compounds are more prevalent in the lichen, consistent with its traditional use for medicinal purposes. This result is consistent with previously published results, suggesting the maximum yield in methanol extract [14]. The concentrated extracts were then used for subsequent phytochemical analysis and biological activity assessments.

3.2. Phytochemical screening.

Phytochemical screening of successive solvent extracts of PF revealed a diverse array of bioactive compounds. The petroleum ether extract predominantly contained nonpolar constituents such as terpenoids and steroids. The chloroform extract exhibited a higher concentration of terpenoids, indicating the presence of moderately polar compounds. In contrast, the acetone and methanol extracts were rich in polar phytochemicals, notably tannins and flavonoids. These findings are consistent with previous reports highlighting the bioactive potential of lichen-derived extracts *PF* [23]. The observed variations in phytochemical composition across different solvent systems underscore the importance of using a range of solvents to achieve comprehensive extraction. Furthermore, the identified phytoconstituents are well documented for their antimicrobial, antioxidant, and anti-inflammatory properties, supporting their relevance for potential therapeutic applications.

3.3. Antibacterial activity.

The antibacterial activity of *PF* extracts was evaluated against *S. aureus* and *E. coli* using the agar well diffusion method. For *S. aureus*, the Gentamicin control disc exhibited a zone of inhibition of 20 mm, confirming its effectiveness as a standard antibacterial agent. In contrast, the chloroform extract showed no inhibition (NI) at any concentration (25 µl, 50 µl, 100 µl), indicating a lack of antibacterial activity.

The acetone extract demonstrated zones of inhibition measuring 14 mm, 12 mm, and 18 mm at 25 µl, 50 µl, and 100 µl, respectively. This indicates moderate antibacterial activity, with the zone of inhibition increasing with concentration. The methanol extract exhibited the most significant activity, with inhibition zones of 14 mm, 18 mm, and 25 mm at 25 µl, 50 µl, and 100 µl, respectively. The efficacy was concentration-dependent, with the highest concentration showing a zone of inhibition comparable to that of Gentamicin. The results, depicted in Figure 1, illustrate the zones of inhibition for each extract and concentration, providing insights into their comparative efficacy (Table 1).

Table 1. Antibacterial effect of *PF* extract against *S. aureus* and *E. coli*.

Standard and PF extracts		**Conc. in µl**		
		25 µl	**50 µl**	**100 µl**
		Zone of inhibition in mm		
Staphylococcus aureus	Gentamicin	**20 mm (10 mcg/ml)**		
	Chloroform	No inhibition	No inhibition	No inhibition
	Acetone	14	12	18
	Methanol	14	18	25
Escherichia coli	Ampicillin	**17 mm (10 mcg/ml)**		
	Chloroform	No inhibition	No inhibition	No inhibition
	Acetone	12	14	24
	Methanol	25	27	29

NI: No Inhibition

For *E. coli*, the Gentamicin control disc produced a zone of inhibition of 17 mm, serving as a benchmark for antibacterial effectiveness. Similar to its effect on *S. aureus*, the chloroform extract exhibited no inhibition (NI) across all concentrations, indicating a lack of antibacterial properties against *E. coli*. The acetone extract showed inhibition zones of 12 mm, 14 mm, and 24 mm for the 25 µl, 50 µl, and 100 µl concentrations, respectively. While the extract's efficacy increased with concentration, its overall activity was lower compared to the methanol extract. The methanol extract demonstrated the highest antibacterial activity, with inhibition zones of 25 mm, 27 mm, and 29 mm at the 25 µl, 50 µl, and 100 µl concentrations, respectively. This extract exhibited superior antibacterial efficacy, particularly at higher concentrations, even surpassing the standard Gentamicin in effectiveness. The results, depicted in Figure 2 illustrate the zones of inhibition for each extract and concentration, providing insights into their comparative efficacy (Table 1).

The results clearly indicate that the methanolic extract of *PF* possesses significant antibacterial activity against both *S. aureus* and *E. coli*, with effectiveness increasing with higher concentrations. These findings are consistent with previously published data [10]. The acetone extract also displayed moderate antibacterial activity, although it was less effective than the methanolic extract. In contrast, the chloroform extract exhibited no antibacterial activity against either bacterial strain, suggesting that the active compounds are more soluble in polar solvents like methanol.

These findings underscore the potential of methanolic extracts of *PF* as a natural antibacterial agent, particularly against common bacterial pathogens. The effectiveness of the

methanol extract is likely due to the presence of high levels of phenolic compounds, such as Physodic acid and Olivetoric acid, and other phytoconstituents known for their antimicrobial properties [24]. This study supports the traditional use of lichen in treating infections and highlights its potential for developing new antibacterial agents.

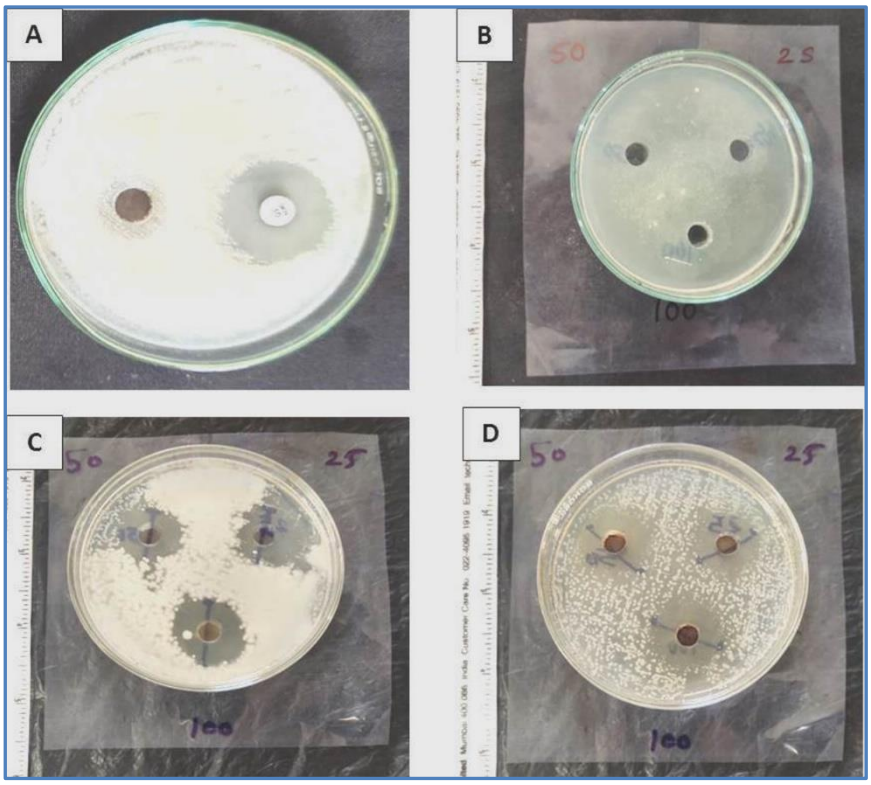

Figure 1. Antibacterial effect of *Pseudevernia furfuracea* extracts against *S. aureus*. **(A)** Gentamicin (positive control); **(B)** Chloroform extract; **(C)** Acetone extract; **(D)** Methanol extract. Zones of inhibition were measured in mm. Abbreviation: NI – No Inhibition.

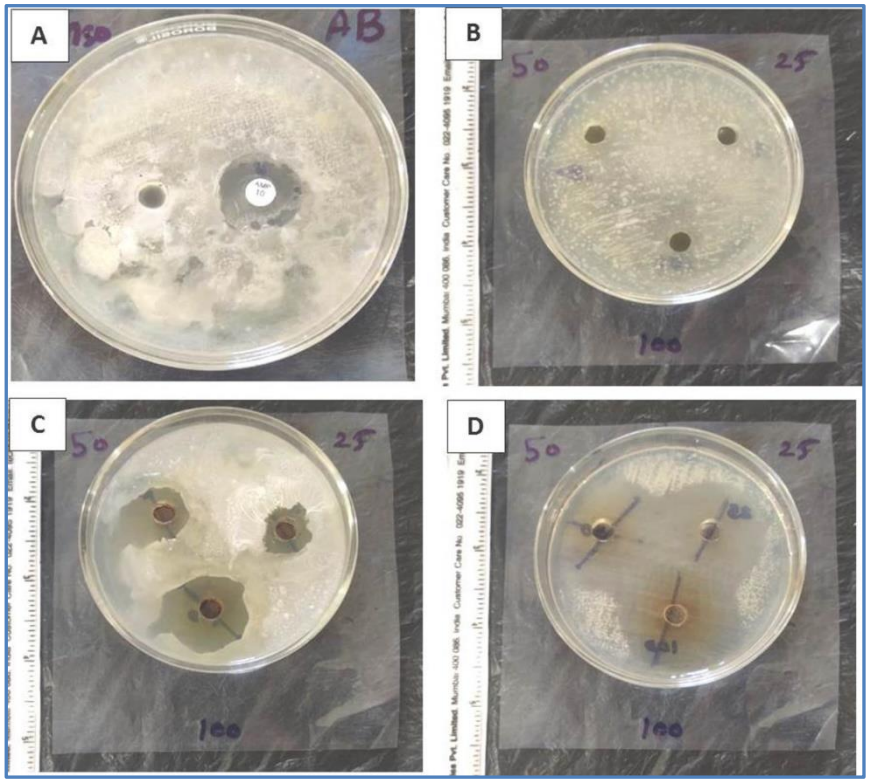

Figure 2. Antibacterial effect of *Pseudevernia furfuracea* extracts against *E. coli*. **(A)** Gentamicin (positive control); **(B)** Chloroform extract; **(C)** Acetone extract; **(D)** Methanol extract. Zones of inhibition were measured in mm. Abbreviation: NI – No Inhibition.

3.4. Molecular docking.

Molecular docking studies were conducted to understand the interaction between the phytoconstituents of *PF* and the bacterial enzyme *E. coli* Gyrase B, a crucial target for antibacterial therapy. In this study, the antibacterial activity of *PF* extracts was evaluated against both *S. aureus* (Gram-positive) and *E. coli* (Gram-negative). However, the molecular docking studies were specifically conducted on *E. coli* Gyrase B, a key bacterial enzyme involved in DNA replication. The rationale for focusing docking studies on E. coli is the critical role of Gyrase B as a well-characterized target for antibacterial agents, particularly in Gram-negative bacteria such as *E. coli*. The availability of high-resolution crystal structures for *E. coli* Gyrase B, combined with its relevance in antibiotic resistance mechanisms, makes it an ideal candidate for in silico studies [25]. Although *S. aureus* was also tested in vitro, the docking studies focused on *E. coli* to provide insights into potential mechanisms of action against this Gram-negative pathogen, which is often more challenging to treat due to its outer membrane barrier.

Table 2. Molecular docking of *PF* phytoconstituents with *E. coli* Gyrase B (PDB ID: 6F86).

Ligand	Docking score	Hydrogen bond interaction	Hydrophobic bond interaction
Native ligand	-8.7	ASP-59, GLU-36	THR-133, ARG-62, VAL-29, VAL-135, ALA-33, PRO-65
Atranorin	-6.7	GLU-36, ARG-62	ASP-59, THR-133, GIH-63, PRO-65, TLE-64
Olivetoric acid	-6.1	GLU-36, ARG-62, GLY-63	THR-133, ILE-64, PRO-65
Chloratranorin	-7.0	THR-133, GLY-63, ASN-32	ASP-59, ILE-64, PRO-65, GLU-36, ASP-35, ALA-39
Depsidone	-5.9	----	ILE-64, GLU-36, ARG-62
Usnic acid	-7.1	GLU-36, ASN-32	ILE-64
Physodallic acid	-8.6	THR-133, ASN-32, GLY-63, GLU-36	ILE-64, ALA-33
Physodic acid	-6.9	ASN-32, ALA-33, ASP-59, THR-133, GIY-63, ABG-64, ILE-62	GLY-81

The docking results and interaction between phytoconstituents indicated favorable binding affinities and interaction for the majority of the tested compounds, as shown in Table 2 and Figures 3 and 4, respectively. Future research could extend molecular docking studies to other key targets specific to Gram-positive bacteria, such as *S. aureus*, to provide a more comprehensive understanding of the lichen's antibacterial mechanisms across different bacterial types.

In our study, we used the native co-crystallized ligand of *E. coli* Gyrase B as a reference, which is a scientifically valid and widely accepted approach. The native ligand provides a biologically relevant benchmark for assessing binding affinity and helps validate the docking protocol. Native Ligand (Binding Energy: -8.7) demonstrates strong binding via hydrogen bonds with ASP A: 59 and THR A: 133, with additional stabilization from GLU A: 36. An unfavorable donor-donor interaction with ARG A: 62 may slightly weaken binding, while Pi-alkyl interaction with PRO A: 65 aids stabilization. Overall, the native ligand presents a well-balanced interaction profile, though optimization is possible at the site of unfavorable interaction. Atranorin (Binding Energy: -6.7) shares similar binding characteristics with the native ligand, forming hydrogen bonds with ASP A: 59, GLU A: 36, and ARG A: 62. A unique interaction with GLY A: 68 distinguishes it, although the absence of alkyl or Pi-alkyl interactions may reduce binding stability (Figure 3).

Olivetoric acid (Binding Energy: -6.1) exhibits key interactions with GLY A: 63, GLU A: 36, and ARG A: 62, similar to the native ligand, with a unique bond to THR A: 133. Its hydrophobic interaction with ILE A: 64 suggests enhanced stabilization, offering a well-

rounded interaction profile. Chloratranorin (Binding Energy: -7.0) forms multiple stabilizing hydrogen bonds with residues like THR A: 133, GLY A: 63, GLU A: 36, and ASN A: 32, along with non-polar interactions with ILE A: 64. This comprehensive profile suggests potentially stronger binding affinity and stability compared to the native ligand (Figure 3) [26].

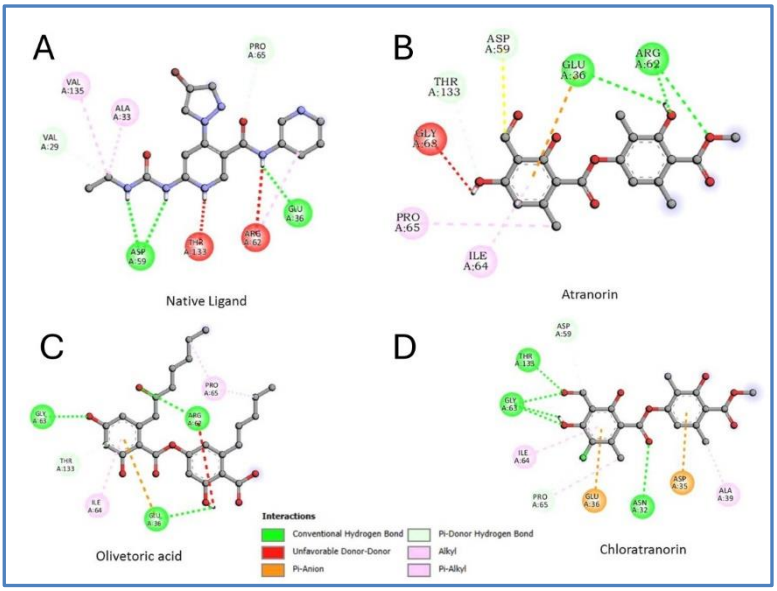

Figure 3. 2D interaction diagrams of docked ligands within the active site of E. coli Gyrase B (PDB ID: 6F86). **(A)** Native ligand (CWW); **(B)** Atranorin; **(C)** Olivetoric acid; **(D)** Chloratranorin. Ligands are shown in ball-and-stick representation, while interacting amino acid residues are depicted in colored circles. Conventional hydrogen bonds are represented by green dashed lines, π-donor hydrogen bonds by light green dashed lines, electrostatic (π-anion) interactions by orange dashed lines, and alkyl and π-alkyl interactions by pink and purple dashed lines, respectively. The interactions illustrate the binding affinity and orientation of the lichen-derived compounds in comparison with the native ligand.

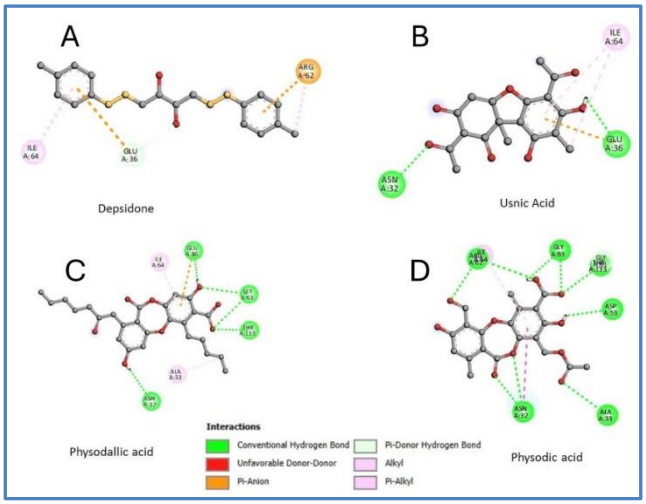

Figure 4. 2D interaction diagrams of docked ligands within the active site of *E. coli* Gyrase B (PDB ID: 6F86). **(A)** Depsidone; **(B)** Usnic acid; **(C)** Physodalic acid; **(D)** Physodic acid. Ligands are shown in ball-and-stick representation, and interacting amino acid residues are highlighted in colored circles. Conventional hydrogen bonds are represented by green dashed lines, π-donor hydrogen bonds by light green dashed lines, electrostatic (π-anion) interactions by orange dashed lines, while alkyl and π-alkyl interactions are shown as pink and purple dashed lines, respectively. These interactions illustrate the binding behavior of the lichen-derived compounds with the target bacterial enzyme.

Depsidone (Binding Energy: -5.9), hydrogen bond with GLU A: 36 and Pi-anion interaction with ARG A: 62, introduces a unique electrostatic component. While simpler than the native ligand, these interactions, particularly with ILE A: 64, may enhance binding through

additional stabilization. Usnic Acid (Binding Energy: -7.1) exhibits stable binding via hydrogen bonds with ASN A: 32 and GLU A: 36. Pi-alkyl interactions with ILE A: 64 contribute to non-covalent stabilization, though the lack of direct interaction with ARG A: 62 may slightly limit binding affinity compared to the native ligand [27].

Physodic acid (Binding Energy: -6.9) shares a key hydrogen bond with ASP A: 59, as seen in the native ligand, with additional bonds to GLY A: 63, THR A: 133, ASN A: 32, and ALA A: 33, enhancing its binding affinity. Pi-donor hydrogen bonds with ALA A: 33 and hydrophobic interactions with ILE A: 64 and ALA A: 54 further stabilize the binding [28]. Physodalic acid (Binding Energy: -8.6) forms critical hydrogen bonds with ASP A: 59, GLY A: 63, THR A: 133, and ASN A: 32, mirroring and exceeding the native ligand's interactions. Pi-donor hydrogen bonds with ALA A: 33 and hydrophobic stabilization with ILE A: 64 and ALA A: 54 suggest a robust binding profile (Figure 4). Overall, the phytoconstituents from *PF*, particularly Physodic and Physodalic acids (as evident from the highest binding energy amongst phytoconstituents), demonstrate strong potential as alternative or complementary ligands to the native compound due to their extensive hydrogen bonding and hydrophobic interactions as compared with previously published data with regard to hydrogen bond interaction [28]. Chloratranorin also shows promise, with a comprehensive interaction profile suggesting higher binding affinity and stability. These findings indicate that these compounds could be further optimized for enhanced efficacy in drug design and are responsible for the antimicrobial potential of the active extracts.

4. Conclusions

This study highlights the significant antibacterial potential of *Pseudevernia furfuracea* (L.), demonstrated through phytochemical analysis, in vitro evaluation, and molecular docking studies. Successive solvent extractions yielded a diverse range of bioactive compounds, with the methanol extract showing a high concentration of polar constituents, including flavonoids and tannins—primarily responsible for the observed antibacterial activity against *S. aureus* and *E. coli*. Molecular docking further supported these findings, showing strong binding affinities of key phytoconstituents to *E. coli* Gyrase B, suggesting a plausible mechanism of action. These results underscore *PF*'s potential as a source of natural antibacterial agents, in line with its traditional medicinal use. Future research should focus on isolating and characterizing individual compounds, evaluating in vivo efficacy and safety, exploring synergistic effects with conventional antibiotics, and optimizing extraction methods. Expanding the antibacterial spectrum could further establish *PF*'s role in pharmaceutical development.

Author Contributions

Conceptualization, S. B.; Methodology, S. B.; Investigation, S. B.; Formal analysis, A. C.; Writing – original draft, D. M.; Writing – review & editing, N. K. and K. B. All authors have read and agreed to the published version of the manuscript.

Institutional Review Board Statement

Not applicable.

Informed Consent Statement

Not applicable.

Data Availability Statement

No new data were created or analyzed in this study. Data sharing is not applicable.

Funding

The authors declare that they have no financial or non-financial interests that could be perceived as influencing the content of this article.

Acknowledgments

The authors would like to thank the Management and Principal of P. Wadhwani College of Pharmacy, Yavatmal, for providing the necessary facilities for the completion of this work.

Conflicts of Interest

The authors declare no conflicts of interest that could have influenced the research or conclusions presented in this manuscript.

References

1. Spribille, T.; Resl, P.; Stanton, D.E.; Tagirdzhanova, G. Evolutionary biology of lichen symbioses. *New Phytol.* **2022**, *234*, 1566-1582, https://doi.org/10.1111/nph.18048.
2. Lõhmus, A.; Motiejūnaitė, J.; Lõhmus, P. Regionally Varying Habitat Relationships in Lichens: The Concept and Evidence with an Emphasis on North-Temperate Ecosystems. *J. Fungi* **2023**, *9*, 341, https://doi.org/10.3390/jof9030341.
3. Kantelinen, A.; Printzen, C.; Poczai, P.; Myllys, L. Lichen speciation is sparked by a substrate requirement shift and reproduction mode differentiation. *Sci. Rep.* **2022**, *12*, 11048, https://doi.org/10.1038/s41598-022-14970-9.
4. Magel, C.L.; Chan, F.; Hessing-Lewis, M.; Hacker, S.D. Differential Responses of Eelgrass and Macroalgae in Pacific Northwest Estuaries Following an Unprecedented NE Pacific Ocean Marine Heatwave. *Front. Mar. Sci.* **2022**, *9*, 838967, https://doi.org/10.3389/fmars.2022.838967.
5. Kello, M.; Goga, M.; Kotorova, K.; Sebova, D.; Frenak, R.; Tkacikova, L.; Mojzis, J. Screening Evaluation of Antiproliferative, Antimicrobial and Antioxidant Activity of Lichen Extracts and Secondary Metabolites In Vitro. *Plants* **2023**, *12*, 611, https://doi.org/10.3390/plants12030611.
6. Kalra, R.; Conlan, X.A.; Gupta, M.; Areche, C.; Bhat, M.; Goel, M. Evaluation of the anticancer potential of secondary metabolites from *Pseudevernia furfuracea* based on epidermal growth factor receptor inhibition. *Nat. Prod. Res.* **2022**, *36*, 6439-6442, https://doi.org/10.1080/14786419.2022.2037587.
7. Toksoz, O.; Turkmenoglu, I.; Berber, D.; Caglayan, P.; Birbir, M.; Sesal, N.C. Evaluation of Antibacterial Potencies of Eight Lichen Extracts Against Gram-Positive Moderately Halophilic Bacteria. *Johns. Matthey Technol. Rev.* **2023**, *67*, 85-96, https://doi.org/10.1595/205651323X16426780863499.
8. Agarwal, T.; Chaudhary, R.K. Unlocking Nature's Aroma: Hora Perfumes and The Art of Harnessing Natural Fragrance Compounds. *Int. J. Adv. Res. Sci. Commun. Technol.* **2023**, *3*, 45–50, https://doi.org/10.48175/IJARSCT-13608.
9. Güvenç, A.; Küpeli Akkol, E.; Süntar, İ.; Keleş, H.; Yıldız, S.; Çalış, İ. Biological activities of *Pseudevernia furfuracea* (L.) Zopf extracts and isolation of the active compounds. *J. Ethnopharmacol.* **2012**, *144*, 726-734, https://doi.org/10.1016/j.jep.2012.10.021.
10. Kosanić, M.; Ranković, B.; Stanojković, T.; Vasiljević, P.; Kočović, A.; Manojlović, A.; Anđić, M.; Bradić, J.; Jakovljević, V.; Manojlović, N. Phytochemical composition, biological activity and anti-inflammatory potential of acetone extract from the lichen *Platismatia glauca* (L.) W.L. Culb. & C.F. Culb. *Nat. Prod. Res.*

2025, *39*, 1111-1121, https://doi.org/10.1080/14786419.2023.2294479.
11. Archana, S.; Keisham, S.S. Bioactive Compounds from Polar Regions: An Account of Chemical Ecology and Biotechnological Applications. *Curr. Org. Chem.* **2022**, *26*, 1055-1087, https://doi.org/10.2174/1385272826666220620152557.
12. Varlı, M.; Pham, H.T.; Kim, S.-M.; Taş, İ.; Gamage, C.D.B.; Zhou, R.; Pulat, S.; Park, S.-Y.; Sesal, N.C.; Hur, J.-S.; Kang, K.B.; Kim, H. An acetonic extract and secondary metabolites from the endolichenic fungus *Nemania* sp. EL006872 exhibit immune checkpoint inhibitory activity in lung cancer cell. *Front. Pharmacol.* **2022**, *13*, 986946, https://doi.org/10.3389/fphar.2022.986946.
13. Mangal, P.; Jha, R.K.; Jain, M.; Singh, A.K.; Muthukumaran, J. Identification and prioritization of promising lead molecules from *Syzygium aromaticum* against Sortase C from *Streptococcus pyogenes*: an *in silico* investigation. *J. Biomol. Struct. Dyn.* **2023**, *41*, 5418-5435, https://doi.org/10.1080/07391102.2022.2086921.
14. Kalra, R.; Conlan, X.A.; Areche, C.; Dilawari, R.; Goel, M. Metabolite Profiling of the Indian Food Spice Lichen, *Pseudevernia furfuracea* Combined With Optimised Extraction Methodology to Obtain Bioactive Phenolic Compounds. *Front. Pharmacol.* **2021**, *12*, 629695, https://doi.org/10.3389/fphar.2021.629695.
15. Dubale, S.; Kebebe, D.; Zeynudin, A.; Abdissa, N.; Suleman, S. Phytochemical screening and antimicrobial activity evaluation of selected medicinal plants in Ethiopia. *J. Exp. Pharmacol.* **2023**, *15*, 51–62, https://doi.org/10.2147/JEP.S379805.
16. Skusa, R.; Groß, J.; Kohlen, J.; Schafmayer, C.; Ekat, K.; Podbielski, A.; Warnke, P. Proof-of-Concept Standardized Approach Using a Single-Disk Method Analogous to Antibiotic Disk Diffusion Assays for Routine Phage Susceptibility Testing in Diagnostic Laboratories. *Appl. Environ. Microbiol.* **2022**, *88*, e00309-00322, https://doi.org/10.1128/aem.00309-22.
17. Balouiri, M.; Sadiki, M.; Ibnsouda, S.K. Methods for *in vitro* evaluating antimicrobial activity: A review. *J. Pharm. Anal.* **2016**, *6*, 71-79, https://doi.org/10.1016/j.jpha.2015.11.005.
18. Arora, S.; Rushiya, P.; Tirpude, K.; Sapkal, N.; Yende, S.; Ittadwar, A.; Shah, S. Exploring the phytoconstituents targeting TNF-α as potential lead compounds to treat inflammatory diseases: an *in-silico* approach. *Digit. Chin. Med.* **2022**, *5*, 264-275, https://doi.org/10.1016/j.dcmed.2022.10.003.
19. Shah, S.; Chaple, D.; Arora, S.; Yende, S.; Mehta, C.; Nayak, U. Prospecting for *Cressa cretica* to treat COVID-19 via *in silico* molecular docking models of the SARS-CoV-2. *J. Biomol. Struct. Dyn.* **2022**, *40*, 5643-5652, https://doi.org/10.1080/07391102.2021.1872419.
20. Arora, S.; Kalpana, T.; Pallavi, R.; Nidhi, S.; Subhash, Y.; Abhay, I.; Sapan, S. Investigation of Neolamarckia cadamba Phytoconstituents Against SARS-CoV-2 3CL Pro: An In-Silico Approach. *Orbital: Electron. J. Chem.* **2023**, *15*, 49-56, https://doi.org/10.17807/orbital.v15i1.17592.
21. Arora, S.; Lohiya, G.; Moharir, K.; Shah, S.; Yende, S. Identification of Potential Flavonoid Inhibitors of the SARS-CoV-2 Main Protease 6YNQ: A Molecular Docking Study. *Digit. Chin. Med.* **2020**, *3*, 239-248, https://doi.org/10.1016/j.dcmed.2020.12.003.
22. Shah, S.; Chaple, D.; Masand, V.H.; Zaki, M.E.A.; Al-Hussain, S.A.; Shah, A.; Arora, S.; Jawarkar, R.; Tauqeer, M. *In silico* study to recognize novel angiotensin-converting-enzyme-I inhibitors by 2D-QSAR and constraint-based molecular simulations. *J. Biomol. Struct. Dyn.* **2024**, *42*, 2211-2230, https://doi.org/10.1080/07391102.2023.2203261.
23. Sarikurkcu, C.; Kocak, M.S.; Calapoglu, M.; Ocal, C.; Tepe, B. Biological and phytochemical evaluation: *Pseudevernia furfuracea* as an alternative multifunctional agent. *J. Funct. Foods* **2016**, *24*, 11-17, https://doi.org/10.1016/j.jff.2016.03.022.
24. Türk, H.; Yılmaz, M.; Tay, T.; Türk, A.Ö.; Kıvanç, M. Antimicrobial Activity of Extracts of Chemical Races of the Lichen Pseudevernia furfuracea and their Physodic Acid, Chloroatranorin, Atranorin, and Olivetoric Acid Constituents. *Z. Naturforsch. C* **2006**, *61*, 499-507, https://doi.org/10.1515/znc-2006-7-806.
25. Michalczyk, E.; Pabiś, M.; Heddle, J.; Ghilarov, D. Structure of *Escherichia coli* DNA gyrase with chirally wrapped DNA supports ratchet-and-pawl mechanism for an ATP-powered supercoiling motor. *bioRxiv* **2024**, 2024-2004, https://doi.org/10.1101/2024.04.12.589215.
26. Oliveira, T.A.d.; Silva, M.P.d.; Maia, E.H.B.; Silva, A.M.d.; Taranto, A.G. Virtual Screening Algorithms in Drug Discovery: A Review Focused on Machine and Deep Learning Methods. *Drugs Drug Candidates* **2023**, *2*, 311-334, https://doi.org/10.3390/ddc2020017.
27. Gallivan, J.P.; Dougherty, D.A. Cation-π interactions in structural biology. *Proc. Natl. Acad. Sci. U.S.A.* **1999**, *96*, 9459-9464, https://doi.org/10.1073/pnas.96.17.9459.
28. Patil, R.; Das, S.; Stanley, A.; Yadav, L.; Sudhakar, A.; Varma, A.K. Optimized Hydrophobic Interactions

and Hydrogen Bonding at the Target-Ligand Interface Leads the Pathways of Drug-Designing. *PLOS ONE* **2010**, *5*, e12029, https://doi.org/10.1371/journal.pone.0012029.

Publisher's Note & Disclaimer